Assessments of Power Systems Voltage Stability Considering Transmission Line Security

Dumrongsak Wongta[1], **Sermsak Uatrongjit**[2],
Chawasak Rakpenthai[3†], and **Nattapong Pothi**[3], Non-members

ABSTRACT

This paper presents two indicators, namely line voltage stability and line ampacity indices, to determine the voltage stability states and line security of power systems under various operating conditions. Both indices rely on the measured values that are already obtained from conventional measurements used in power systems. The identification of weak buses and critical lines based on the proposed indices is possible using only voltage magnitude and real power measurements. To validate the effectiveness of the proposed indices, two power networks have been tested under increasing system loading and line outage conditions. Numerical experimental results indicate that by considering both line voltage stability and line ampacity indices, power systems could mitigate the risks of voltage collapse and excessive current in transmission line.

Keywords: Line Ampacity, Voltage Stability, Critical Line, Transmission Line Security, Line Outage

1. INTRODUCTION

As electrical energy consumption and the integration of renewable sources continue to rise, operation of power system has become a complex task involving both economic and security constraints. The disturbances in power system, such as a sudden increase in load, transmission line outage, generator failure, and the intermittent nature of renewable energy sources, have the potential to reduce the voltage stability margin. Consequently, the maximum power that can be supplied to the load bus without breaching voltage limits also diminishes. Without appropriate estimation and mitigation strategies for the voltage stability problem, voltage collapse may occur in power system which can result in severe damage to the network [1] and potentially lead to an electrical blackout. Thus, the assessment of the voltage stability in power systems under various operating conditions become of utmost importance. Several voltage stability indicators, which play essential roles in identifying critical locations within power networks from where voltage collapse may originate, have been developed. Voltage stability indices based on the maximum loading conditions of a two-bus system have been presented in [2]-[7]. The transmission line parameters and some system variables such as bus voltages and power flow through lines are used to formulate the indices. These indicators require minimal computational effort, making them suitable for rapid identification of systems operating under changing loads and contingency conditions. However, due to some assumptions in these indices, different and unpredictable values can be obtained when they are applied to large-scale power networks [8]-[10]. Other indices based on Jacobian matrix of load flow analysis have been presented in [11]-[14]. An index based on the minimum singular value decomposition of the Jacobian matrix has been presented in [11]. The maximum singular value of the inverse Jacobian matrix and its derivative has been presented in [12]. This index is approximately linear and can determine the voltage stability margin. A model analysis-based index based on the minimum eigenvalue and right eigenvector of the Jacobian matrix has been presented in [13]. The voltage stability of system occurs when all eigenvalues are positive. The maximum element of system tangent vector, which are the sensitivity of state variables including the bus voltage magnitudes and angles with respect to the load variation, has been presented in [14]. The inverse of the maximum element of the tangent vector is close to zero at the voltage collapse point. A test function based on the reduction of the Jacobian matrix with respect to the critical bus of system has been presented in [15]. This index can be used to predict the voltage collapse point by fitting the test function using a quadratic model. Test results in [15] also show that the minimum singular value and the eigenvalue of Jacobian matrices proposed in [11] and [13] are not good indicators due to their nonlinear behaviors when the bus voltage magnitude approaches its collapse point. In addition, these techniques require rather time consuming computation steps and may not be suitable for implementation in realistic power systems because accurate parameters are required for system models. In [16]-[22], indices based on Thévenin equivalent impedance of

Manuscript received on October 11, 2023; revised on March 17, 2024; accepted on April 10, 2024. This paper was recommended by Associate Editor Komsan Hongesombut.

[1]The author is with Department of Electrical Engineering, Faculty of Engineering, Chiangrai College, Thailand.

[2]The author is with Department of Electrical Engineering, Faculty of Engineering, Chiang Mai University, Thailand.

[3]The authors are with Department of Electrical Engineering, School of Engineering, University of Phayao, Thailand.

[†]Corresponding author: chawasak@hotmail.com

Digital Object Identifier: 10.37936/ecti-eec.2024222.251256

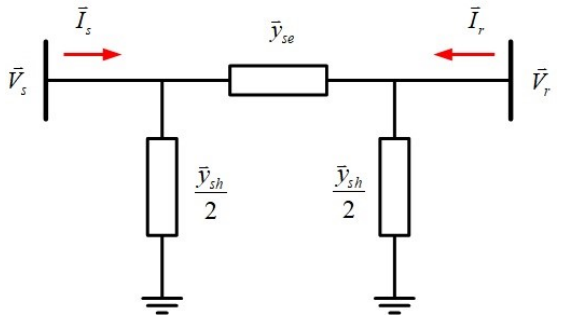

***Fig. 1**: Equivalent π circuit of transmission line.*

the rest of the power system using the data obtained from the measurement system, have been presented for real-time voltage stability assessment. The external Thévenin equivalent impedance has the same magnitude as the load impedance at the bus when the maximum loading condition occurred. The point of voltage collapse is also the system operating point, at which the maximum available power can be delivered to the load. The voltage stability of bus installed phasor measurement units (PMUs) can be determined. A systematic qualitative and quantitative comparison of some voltage stability indices based on the Thévenin equivalent obtained from estimated states using both conventional and PMU measurements has been performed and reported in [23].

In practice, the maximum available power flowing through the transmission line connecting the sending bus and the receiving bus depends on the operating limit of the transmission line. The current magnitude of the conductor must not exceed the line ampacity or line rating to prevent excessive conductor temperature [24]-[26]. Transmission line security is determined by its thermal security limit, ensuring that the magnitude of current flowing through the line is within its ampacity or current rating. Consequently, power system analysis under the occurrence of disturbances should estimate or predict not only the voltage stability of the load bus, but also the security of the transmission line. By using the maximum available loading margin, which satisfies both the voltage stability and line security conditions, it becomes possible to maintain the voltage stability of buses and prevent any potential damage to transmission lines.

In this paper, assessment of voltage stability considering the thermal security of each transmission line in power systems is proposed. The main contributions of this work can be summarized as follows:

(A) Two indices that can be used to estimate or predict the voltage stability and the line's thermal security levels have been proposed. The maximum load demand, which preserves the operation of the power system within the voltage stability and line security regions, is a critical loading condition.

(B) The proposed indices use only bus voltage magnitudes and real power flow measurements to compute their values during on-line power system operations. They are conventional measuring devices used in power systems. Phase angle measurement is not required.

The paper is organized as follows: The power flow equations for a transmission line connected between two buses and conventional voltage stability indices are described in Section 2. The proposed indices developed to assess voltage stability and line ampacity levels are explained in the next section. Numerical results on two test systems are illustrated in Section 4. Finally, conclusions are given in the last section.

2. RELATED BACKGROUND

2.1 Power Flow Formulation

In this subsection, the power flow equations, which are used to develop voltage stability indices, are described. Fig. 1 shows an equivalent π circuit of transmission line. The branch current phasor flowing from bus s to bus r can be obtained by

$$\vec{I}_s = \left(\frac{1}{2}\vec{y}_{sh} + \vec{y}_{se}\right)\vec{V}_s - \vec{y}_{se}\,\vec{V}_r, \tag{1}$$

where
$\vec{I}_s = I_s\angle\theta_s$ is the current phasor at the sending end bus,
$\vec{V}_s = V_s\angle\delta_s$ and $\vec{V}_r = V_r\angle\delta_r$ are voltage phasor at the sending end bus and the receiving end bus, respectively,
$\vec{y}_{se} = g_{se} + jb_{se}$ denotes a series admittance of transmission line, and
$\vec{y}_{sh} = g_{sh} + jb_{sh}$ denotes a shunt admittance of transmission line. It is usually assumed that g_{sh} is zero.
A complex power flowing from the sending bus s to the receiving bus r, $\vec{S}_s$, can be calculated by

$$\vec{S}_s = P_s + jQ_s = \vec{V}_s\,\vec{I}_s^{\,*}, \tag{2}$$

where P_s and Q_s are the real and reactive power flow from bus s to bus r, respectively. Note that the superscript * denotes a complex conjugation. Substituting (1) into (2), and separating into real and imaginary part, one obtains

$$P_s = g_{se}V_s^2 - V_sV_r\left(g_{se}\cos\delta + b_{se}\sin\delta\right), \tag{3}$$

$$Q_s = -\left(\frac{1}{2}b_{sh} + b_{se}\right)V_s^2 + V_sV_r\left(b_{se}\cos\delta - g_{se}\sin\delta\right), \tag{4}$$

where $\delta = \delta_s - \delta_r$ and g_{sh} is assumed to be zero.

Similarly, the power flow from bus r to s can be computed by

$$P_r = g_{se}V_r^2 - V_sV_r\left(g_{se}\cos\delta - b_{se}\sin\delta\right), \tag{5}$$

$$Q_r = -\left(\frac{1}{2}b_{sh} + b_{se}\right)V_r^2 + V_sV_r\left(b_{se}\cos\delta + g_{se}\sin\delta\right), \tag{6}$$

where P_r and Q_r are the real and reactive power flow from bus r to bus s, respectively.

2.2 Conventional Voltage Stability Indices

Some conventional voltage stability indices based on bus voltage phasor, power flow, and transmission line parameters are briefly reviewed in this sub-section. The values of these indices vary between 0 and 1. Usually, the values must be less than 1 to ensure a stable power system operation.

Fast Voltage Stability Index (FVSI):

A fast voltage stability index, FVSI, developed based on voltage collapse occurrence at contingency condition is proposed in [3]. The formulation of the FVSI is given by,

$$FVSI = \frac{-4\left|z_{se}\right|^2 Q_r}{x_{se}{V_s}^2}, \tag{7}$$

where $z_{se} = r_{se} + jx_{se}$ is a series impedance of transmission line.

Line Stability Index (L_{mn}):

A line stability index, L_{mn}, is presented in [5]. It is based on the concept of power transfer in a single transmission line. The proposed index is given by:

$$L_{mn} = \frac{-4x_{se}Q_r}{{V_s}^2 \sin^2(\theta - \delta)}, \tag{8}$$

where $\theta = \tan^{-1}(x_{se}/r_{se})$ is a series impedance angle of transmission line.

Line Stability Factor (L_{QP}):

A line stability factor, L_{QP}, is proposed based on basic power flow equations on a single transmission line model [28]. This index is expressed as

$$L_{QP} = 4\left(\frac{x_{se}}{{V_s}^2}\right)\left(\frac{x_{se}}{{V_s}^2}P_s^2 + Q_r^2\right). \tag{9}$$

New Line Voltage Stability Index (BVSI):

A new line voltage stability index, BVSI, is derived using the concept of power flow though a single transmission line connected between two buses [9]. The BVSI is obtained as follows,

$$BVSI = \frac{-4r_{se}\left|z_{se}\right|^2 P_r}{V_s^2(r_{se}\cos\delta + x_{se}\sin\delta)^2}. \tag{10}$$

These conventional voltage stability indices can be applied to evaluate voltage stability levels in either off-line or on-line operations of power systems. However, for on-line assessments, each index needs different measuring values. Some may require phase angle measurements. In addition, their performances depend on the network's configuration and operating conditions [7]- [10].

3. PROPOSED ASSESSMENT APPROACH

In this section, two indicators are proposed for assessing the voltage stability and line security of power networks. They are derived based on the real power flow through the transmission line and bus voltage magnitudes. The maximum loading condition that satisfies the limit of either indicator can be considered as a critical loading condition.

3.1 Line Voltage Stability Index

The voltage stability depends on influence of the power loading at the load bus. By considering the power flow from bus r to bus s, we can re-arrange (5) and formulate a quadratic equation in terms of a variable V_r as

$$g_{se}V_r^2 - KV_sV_r - P_r = 0, \tag{11}$$

where $K = g_{se}\cos\delta - b_{se}\sin\delta$. The roots of (11) are obtained as,

$$V_r = \left(KV_s \pm \sqrt{K^2V_s^2 + 4g_{se}P_r}\right) \Big/ 2g_{se}, \tag{12}$$

Since the voltage magnitude V_r is a real number, the discriminant must satisfy the following condition,

$$K^2V_s^2 + 4g_{se}P_r \geq 0. \tag{13}$$

Moreover, (5) can be re-arranged as

$$V_s\left(g_{se}\cos\delta - b_{se}\sin\delta\right) = KV_s = \left(g_{se}V_r^2 - P_r\right)/V_r. \tag{14}$$

Substituting (14) into (13), then we can define a line voltage stability index (LVSI) as the follows

$$LVSI = \frac{-4g_{se}V_r^2P_r}{(g_{se}{V_r}^2 - P_r)^2} \leq 1\,. \tag{15}$$

The value of LVSI closes one when the voltage magnitude at the receiving end bus approaches the voltage collapse point. The proposed LVSI requires only measurements of the bus voltage magnitude and the real power flow to determine voltage stability level under various operating conditions of power system.

3.2 Line Ampacity Index

Considering Fig. 1, the real power loss of the transmission line can be obtained as follows

$$P_s + P_r = I_{se}^2 r_{se}, \tag{16}$$

where I_{se} is the magnitude of series current phasor of the line, and $r_{se} = g_{se}/(g_{se}^2 + b_{se}^2)$ represents line series resistance.

Substituting (3) and (5) into (16), one obtains

$$I_{se}^2 r_{se} = g_{se}\left(V_s^2 + V_r^2\right) - 2g_{se}V_sV_r\cos\delta. \tag{17}$$

By using trigonometric identity, (5) can be re-written as

$$P_r = g_{se}V_r^2 - V_sV_r(g_{se}\cos\delta \pm b_{se}\sqrt{1 - \cos^2\delta}). \tag{18}$$

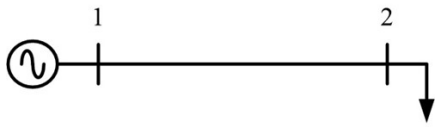

***Fig. 2**: Single line diagram of 2-bus system.*

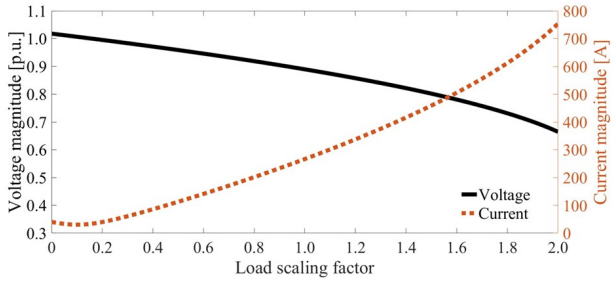

***Fig. 3**: Voltage and current magnitudes for 2-bus system.*

Since $K = (g_{se}V_r^2 - P_r)/V_sV_r$, (18) can be re-arranged into the following equation

$$y_{se}^2 \cos^2\delta - 2b_{se}K\cos\delta + \left(K^2 - b_{se}^2\right) = 0, \qquad (19)$$

where $y_{se}^2 = g_{se}^2 + b_{se}^2$ is the squared magnitude of line's series admittance. Two values of $\cos\delta$ are obtained from (19). The one with larger magnitude is chosen since the phase difference of bus voltages phasors of the line is generally small. Hence, we obtain

$$\cos\delta = \left(g_{se}K + \left|b_{se}\right|\sqrt{y_{se}^2 - K^2}\right) \Big/ y_{se}^2. \qquad (20)$$

Substituting (20) into (17), a series current magnitude flowing along transmission line can be expressed as

$$I_{se}^2 = y_{se}^2\left(V_s^2 + V_r^2\right) - 2V_sV_r\left(g_{se}K + \left|b_{se}\right|\sqrt{y_{se}^2 - K^2}\right). \qquad (21)$$

From (21), we propose a line ampacity index (LAI) as

$$LAI = I_{se}/I_{cr} \le 1, \qquad (22)$$

where I_{cr} is the current rating of transmission line. The value of LAI must be less than unity to maintain thermal security of transmission line. The index value reaches one when the transmission line operates at its maximum loading condition. The proposed LAI requires onlymeasurements of the bus voltage magnitudes and the real power flow to determine the security status of each line of power system. Critical line can also be identified based on the proposed index for power system operation under variations in loading and contingency.

4. CASE STUDIES AND RESULTS

In this section, the proposed assessment approach is demonstrated using two test systems. For each transmission line, the voltage stability and line ampacity

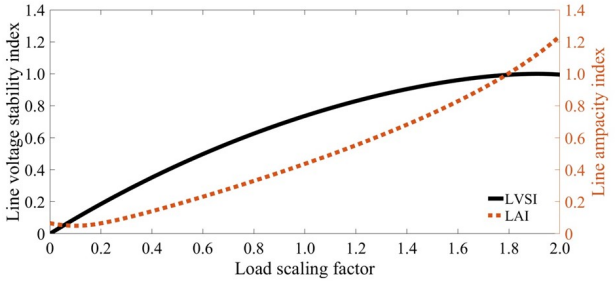

***Fig. 4**: LVSI and LAI for 2-bus system.*

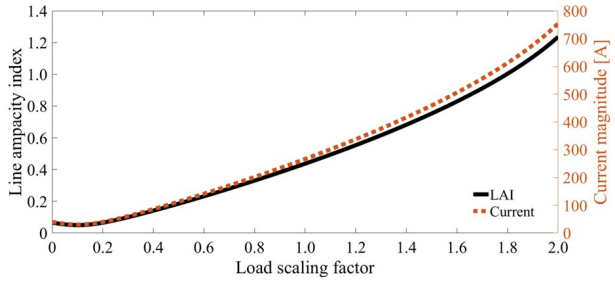

***Fig. 5**: LAI and current magnitude for 2-bus system.*

indices proposed in the previous section are computed under various loading conditions. Both real and reactive powers at the base load are multiplied by a load scaling factor to simulate loading variation. The scaling factor is increased until the voltage collapse state occurs. The operating states of the test systems are simulated by using MATPOWER [27].

4.1 2-Bus System

Fig. 2 shows a 2-bus system operated at 500 kV with a double-circuit transmission line. The line's length is set to 180 km and the phase conductor is assumed to be Hawk conductor. The real and reactive power loads at the receiving end are 340 MW and 285 Mvar, respectively. The voltage magnitude at the sending bus is fixed to be 1 p.u. while the voltage magnitude at the receiving bus depends on the loading conditions. Fig. 3 illustrates the voltage magnitude at the receiving bus and the series current magnitude on the phase conductor as functions of the load scaling factor. As the load increases, the current magnitude rises while the voltage magnitude declines. Although, as shown in the figure, the voltage collapse point occurs when the load scaling factor is 2, the current magnitude flowing though the conductor is approaching its current rating, that is 610 A, when the load scaling factor closes to 1.796. Therefore, the critical load scaling factor for this situation is 1.796 to ensure transmission line security, as the current magnitude through the phase conductor remains below its current limit.

Fig. 4 shows the bus voltage magnitude, the proposed voltage stability index (LVSI), and the line ampacity index (LAI) of line with increasing load scaling factor. It can be observed that the value of the voltage stability

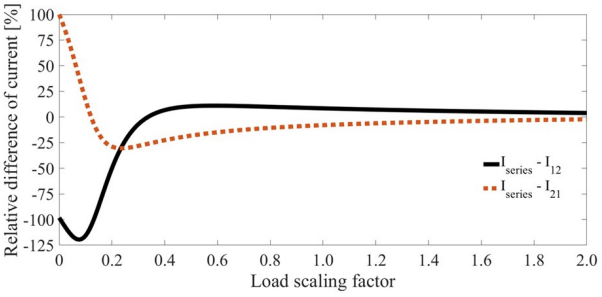

***Fig. 6**: Difference of current magnitudes for 2-bus system.*

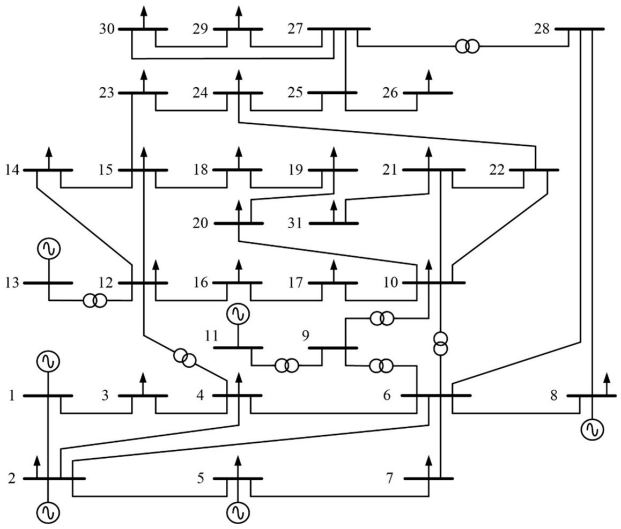

***Fig. 7**: Single line diagram of IEEE 30-bus system.*

index increases from 0 to 1 as load increases. The LVSI reaches its maximum value of 1 at the point of voltage collapse. Likewise, the value of the LAI also rises with an increase in loading. At the critical load scaling factor of 1.796, the LAI is equal to 1 where the current magnitude of the phase conductor is equal to the current rating. Fig. 5 shows the relationship between the LAI and the series current magnitude as functions of the load scaling factor for the 2-bus system. The value of LAI approaches unity when the series current magnitude is close to the current rating of the transmission line. Fig. 6 displays the percentage difference between the branch current magnitudes (I_{12} and I_{21}), which also includes effects of the series and shunt admittances, and the series current magnitude (I_{series}), which considers only the series admittance of the transmission line. For large loads, where a significant proportion of the branch current is contributed by the series current phasors, the difference tends to zero. This implies that using direct measurement of the branch current magnitude at each line terminal causes an enormous error in ampacity and power loss estimation of the transmission line.

***Table 1**: LVSI and LAI for IEEE 30-bus system.*

Line		Case 1 $\lambda = 3.0021$		Case 2 $\lambda = 1.8721$	
From	to	LVSI	LAI	LVSI	LAI
1	2	0.0979	0.1048	0.3753	0.4795
1	3	0.2465	0.0976	0.5762	0.2757
2	4	0.2126	0.0884	0.4287	0.1921
3	4	0.0574	0.0926	0.1679	0.2597
2	5	0.2056	0.0659	0.3910	0.1422
2	6	0.2880	0.1159	0.5379	0.2482
4	6	0.0935	0.1300	0.1794	0.2573
5	7	0.1277	0.0747	0.2573	0.1507
6	7	0.0296	0.0232	0.0384	0.0253
6	8	0.0793	0.1326	0.1444	0.2540
8	28	0.0194	0.0156	0.0811	0.0394
6	28	0.0610	0.0571	0.0729	0.0667
10	17	0.0217	0.3115	0.0751	0.7007
10	20	0.1018	0.3060	0.2555	0.7154
10	21	0.0072	0.1250	0.0770	0.7898
10	22	0.0252	0.2052	0.0448	0.6180
12	14	0.1223	0.2565	0.2397	0.5079
12	15	0.1169	0.4846	0.2408	**1.0000**
12	16	0.1534	0.4063	0.2145	0.5789
14	15	0.0060	0.0156	0.0023	0.0748
16	17	0.0978	0.2600	0.1126	0.3036
15	18	0.1662	0.3964	0.2436	0.5993
15	23	0.1292	0.2935	0.1034	0.4837
18	19	0.0681	0.2585	0.0874	0.3260
19	20	0.0217	0.2158	0.0715	0.5270
21	22	0.0317	0.4516	0.0404	0.8595
22	24	0.0443	0.2828	0.0570	0.5820
23	24	0.1770	0.3918	0.1549	0.3535
24	25	0.0779	0.2055	0.1592	0.2885
25	26	0.1085	0.1804	0.2070	0.3514
25	27	0.0112	0.2582	0.2316	0.5198
27	29	0.4781	0.7546	0.3610	0.5375
27	30	0.7646	**1.0000**	0.5488	0.6154
29	30	0.4897	0.6383	0.2708	0.3262

4.2 IEEE 30-Bus System

In this subsection, the standard IEEE 30-bus system has been modified as the test system. As shown in Fig. 7, the system consists of 6 generators, 7 transformers, 41 lines, and 24 loads. Single-and double-circuit transmission lines are employed for 33 kV and 132 kV overhead lines, respectively. One conductor per phase is assumed except for line 21-22, where two conductors per phase are employed to enhance the line's carrying capacity. The phase conductors of the 33 kV and 132 kV overhead lines are assumed to be Panther and Hawk conductors, respectively. The line's length is chosen based on positive sequence reactance. Three test cases are considered to verify the effectiveness of the proposed indices under various loading conditions.

Case 1: This case tests the load variation at a single load bus. Both real and reactive powers at bus 30 are increased until voltage collapse occurs.

Case 2: Both real and reactive powers at all load buses are increased until voltage collapse occurs.

Case 3: This is similar to Case 2, however, single transmission lines' outage is also considered.

From the experimental results, it is found that the critical load scaling factors of case 1 and 2 are 3.0021 and

1.8721, respectively. Table 1 shows the LVSI and LAI obtained at the critical loading conditions of the IEEE 30-bus system. It can be seen that line 27-30 and line 12-15 are the critical lines of cases 1 and 2, respectively, because their line ampacity indices are 1. A line with a high value of the LVSI can be considered as weak line in terms of the voltage stability. Such a line poses a risk of voltage instability for the connected buses, potentially leading to voltage instability issues. In addition, a line with a high value of the LAI can be considered as weak security line because its operating point may be near the thermal limit of the phase conductor.

Figs. 8 and 9 show, for case 2, the variation of the LVSI and LAI of line 27-30 and line 12-15 under increasing of loads, respectively. From the results in Fig. 8, it can be seen that the value of the LVSI rises to 1 when the voltage magnitude at bus 30 reaches the point of voltage collapse. However, because the LAI approaches 1 as the load scaling factor approaches 3, the maximum loading at bus 30 must be restricted to 3 times of base load. The results in Fig. 9 also indicates that the value of LVSI of line 12-15 is less than one. This implies that the voltage collapse condition cannot occur at both bus 12 and bus 15 in this test case. However, because the value of LAI is close to 1 when the load scaling factor closes to 1.870, the maximum loading is limited to 1.870 times of base load for case 2. This test result highlights the fact that increasing the load in power systems may be limited by transmission line security. The magnitude of the current flowing through the phase conductor may reach the current rating of the conductor before bus voltage collapse occurs.

For case 3, the results of the single line outage analysis of the IEEE 30-bus system are summarized in Table 2. The maximum load scaling factor for the IEEE 30-bus system under each line outage case is given. The critical lines in this test case are also identified based on the LAI, where the series current in phase conductor reaches its line ampacity before voltage collapse occurs. Nevertheless, in some case, a voltage collapse occurs before there is excess current in the transmission line. The results in Table 2 indicate that as the outage of line 27-29 happens, the LVSI of line 27-30 is high when system loading is increased. Hence, bus 30, which is a load bus, can be considered as a weak bus under this test condition.

4.3 Effect of Measurement Noise

The measured values of the bus voltage magnitude and real power flow obtained from each substation typically contain measurement noise. To investigate the influence of the measured values on the proposed indices, both real and reactive powers at all load buses are increased by 1.80 time of the base load. In this study, even though the measured values used to determine the proposed indices can be obtained from both PMU and RTU devices, it is assumed that the measuring values are obtained solely from RTU devices. The maximum uncertainties of the voltage magnitude and power flow measurements

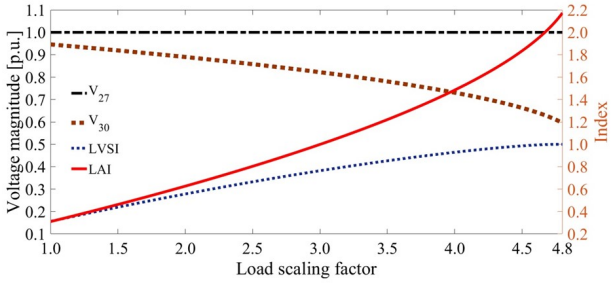

***Fig. 8**: LVSI and LAI of line 27-30 for case 2.*

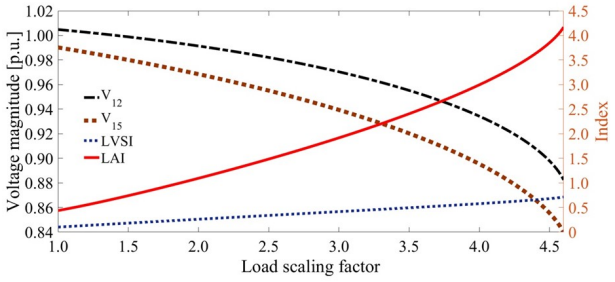

***Fig. 9**: LVSI and LAI of line 12-15 for case 2.*

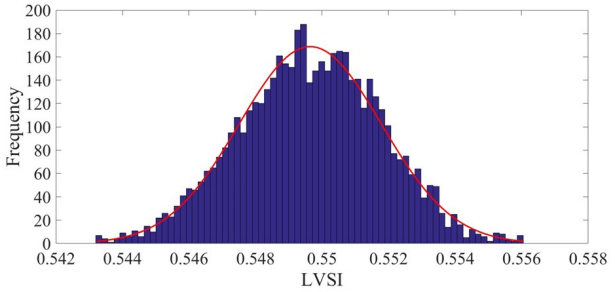

***Fig. 10**: LVSI histogram of line 1-3 for IEEE 30-bus system.*

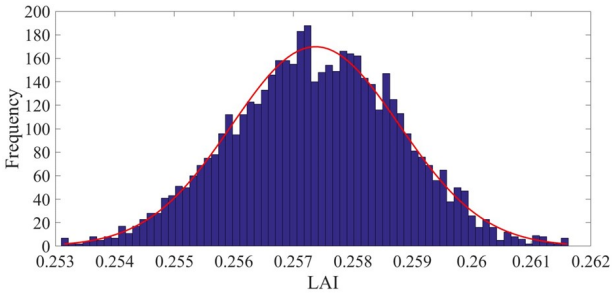

***Fig. 11**: LAI histogram of line 1-3 for IEEE 30-bus system.*

are assumed to be 0.4% and 1.0%, respectively. For each measurement, zero-mean Gaussian noise with a corresponding standard deviation is added. Testing has been performed using 5,000 Monte Carlo simulations. From the experimental results in this test case, it is found that the largest LVSI occurs at line 1-3 while the largest LAI occurs at line 12-15.

***Table 2**: Maximum loading and critical line for IEEE 30-bus system under line outage conditions.*

Line outage	λ_{max}	Critical line	LAI	LVSI
1-3	1.8949	12-15	1.0000	0.2413
12-15	1.0713	21-22	1.0000	0.0368
23-24	1.9098	10-21	1.0000	0.1011
27-29	1.4701	27-30	1.0000	0.7636

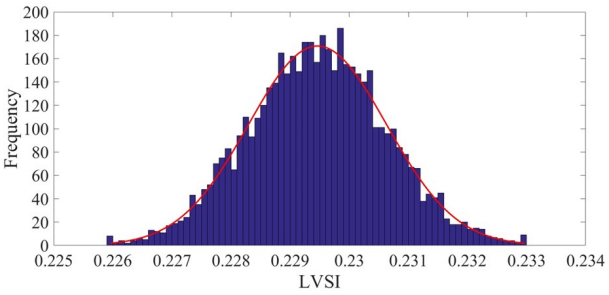

***Fig. 12**: : LVSI histogram of line 12-15 for 30-bus system.*

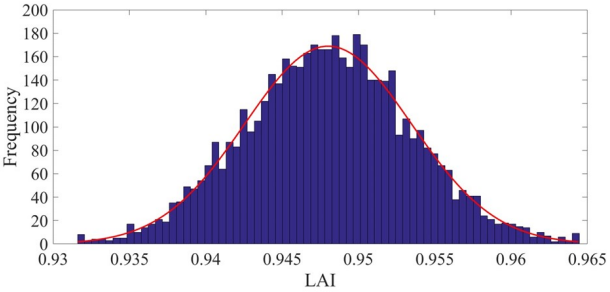

***Fig. 13**: LAI histogram of line 12-15 for 30-bus system.*

Figs. 10 and 11 show histograms of the LVSI and LAI computed using the measurements corresponding to line 1-3, respectively. Bus 1 is a generator bus, while the load bus 3 can be considered as a weak bus because its LVSI is greater than 0.50. However, the line 1-3 has a high security level since its LAI value is less than 0.30. The standard deviations of the LVSI and LAI obtained from line 1-3 are 0.19% and 0.27%, respectively. Figs. 12 and 13 show histograms of the LVSI and LAI of line 12-15 under this test condition, respectively. Bus 15 whose LVSI is less than 0.25 is a strong voltage bus, whereas bus 12 is a voltage-controlled bus. However, line 12-15 has a low security level because its LAI value is near unity. The standard deviations of LVSI and LAI for line 12-15 are 0.25% and 0.28%, respectively.

It can be seen that the values of LVSI and LAI obtained using the conventional measurements have small percentage of standard deviations. Consequently, the proposed indices can be applied to a real-time system to determine or monitor the voltage stability and security levels of each line.

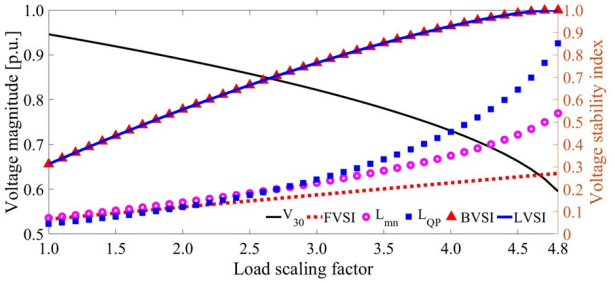

***Fig. 14**: Comparison of various voltage stability indices of line 27-30 for IEEE 30-bus system (Case 1).*

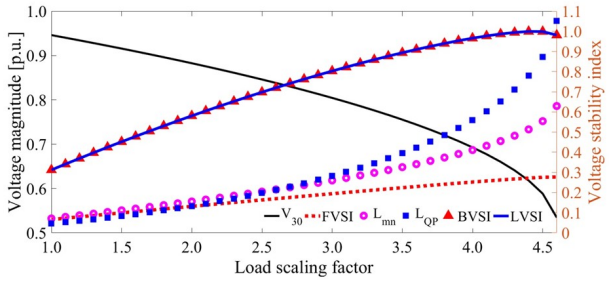

***Fig. 15**: Comparison of various voltage stability indices of line 27-30 for IEEE 30-bus system (Case 2).*

***Table 3**: Measuring values of stability indices.*

Indices	Measurements
FVSI [3]	V_s , Q_r
L_{mn} [5]	V_s , δ_s , δ_r , Q_r
L_{QP} [28]	V_s , P_s , Q_r
BVSI [9]	V_s , δ_s , δ_r , P_r
Proposed LVSI, LAI	V_s , V_r , P_r

4.4 Comparisons with Conventional Voltage Stability Indices

In this subsection, the proposed LVSI has been compared with other voltage stability indices, that is, FVSI [3], L_{mn} [5], L_{QP} [28], and BVSI [9], under the loading conditions of the IEEE 30-bus system. The measuring values that are required to calculate these indices are summarized in Table 3. It should be noted that the measured values for the proposed LVSI can be employed to evaluate transmission line security level as well.The testing conditions of case 1 and case 2 of subsection 4.2 are used to validate the performance of the indices. The values of these voltage stability indices must be less than 1.0 to maintain the voltage stability of the corresponding bus. Line 27-30 is a critical line and bus 30 is a weak bus for both test cases. The comparison results for case 1 and case 2 of the IEEE 30-bus system are shown in Figs. 14 and 15, respectively. It can be observed that the proposed LVSI and BVSI can successfully determine the point of voltage collapse. LVSI provides voltage

stability assessment similar to that of BVSI. Nevertheless, since phase difference between the sending and receiving bus voltage phasors are required to compute BVSI, these measurements are obtained via phase measuring device, such as PMU. By contrast, FVSI, L_{mn}, and L_{QP} fail to identify the collapse point. In Case 1, voltage collapse occurs before the values of FVSI, L_{mn}, and L_{QP} are close to 1. In Case 2, voltage collapse occurs before the values of FVSI and L_{mn} are close to 1, whereas the L_{QP} value is 1 before voltage collapse occurs.

5. CONCLUSION

In this paper, two indices derived based on real power flow and real power loss of a transmission line have been proposed to assess voltage stability and line ampacity levels of power systems. A technique based on a quadratic equation to estimate phase angle difference has been provided to avoid phase angle measurements. Therefore, the proposed indices use only bus voltage magnitudes and real power flow measurements obtained from common RTUs to assess the voltage stability and line security states of power systems under different operating conditions. The results obtained from two test power networks show that the proposed line voltage stability index can determine the voltage collapse point and weak buses whereas the proposed line ampacity index can determine the critical and weak security lines.

ACKNOWLEDGEMENT

This work was supported by the Thailand Science Research and Innovation (TSRI) under Grant RSA6180022.

REFERENCES

[1] T. Van Cutsem and C. Vournas, *Voltage Stability of Electrical Power Systems*, New York: Springer Science, 1998.

[2] P. Kessel and H. Glavitsch, "Estimating the voltage stability of a power system," *IEEE Transactions on Power Delivery*, vol. 1, no. 3, pp. 346-354, Jul. 1986.

[3] I. Musirin and T. K. Abdul Rahman, "Novel fast voltage stability index (FVSI) for voltage stability analysis in power transmission system," in *Student Conference on Research and Development*, Shah Alam, Malaysia, 2002, pp. 265-268.

[4] I. Musirin and T. K. Abdul Rahman, "Estimating maximum load ability for weak bus identification using FVSI," *IEEE Power Engineering Review*, vol. 22, no. 11, pp. 50-52, Nov. 2002.

[5] V. Balamourougan, T. S. Sidhu, and M. S. Sachdev, "Technique for online prediction of voltage collapse," *IEE Proceedings - Generation, Transmission and Distribution*, vol. 151, no. 4, pp. 453-460, Jul. 2004.

[6] A. Yazdanpanah-Goharrizi and R. Asghari, "A novel line stability index (NLSI) for voltage stability assessment of power systems," in *Proceedings of the 7th WSEAS International Conference on Power Systems*, Beijing, China, 2007, pp. 164-167.

[7] R. Tiwari, K. R. Niazi, and V. Gupta, "Line collapse proximity index for prediction of voltage collapse in power systems," *International Journal of Electrical Power & Energy Systems*, vol. 41, no. 1, pp. 105-111, Oct. 2012.

[8] S. Ratra, R. Tiwari, and K. R. Niazi, "Voltage stability assessment in power systems using line voltage stability index," *Computers & Electrical Engineering*, vol. 70, pp. 199-211, Aug. 2018.

[9] B. Ismail *et al.*, "New line voltage stability index (BVSI) for voltage stability assessment in power system: the comparative studies," *IEEE Access*, vol. 10, pp. 103906-103931, Sep. 2022.

[10] S. Mokred, Y. Wang, and T. Chen, "Modern voltage stability index for prediction of voltage collapse and estimation of maximum load-ability for weak buses and critical lines identification," *International Journal of Electrical Power & Energy Systems*, vol. 145, 108596, Feb. 2023.

[11] P. A. Lof, T. Smed, G. Andersson, and D. J. Hill, "Fast calculation of a voltage stability index," *IEEE Transactions on Power Systems*, vol. 7, no. 1, pp. 54-64, Feb. 1992.

[12] A. Berizzi, P. Finazzi, D. Dosi, P. Marannino, and S. Corsi, "First and second order methods for voltage collapse assessment and security enhancement," *IEEE Transactions on Power Systems*, vol. 13, no. 2, pp. 543-551, May 1998.

[13] B. Gao, G. K. Morison, and P. Kundur, "Voltage stability evaluation using modal analysis," *IEEE Transactions on Power Systems*, vol. 7, no. 4, pp. 1529-1542, Nov. 1992.

[14] A. C. Z. De Souza, C. A. Canizares, and V. H. Quintana, "New techniques to speed up voltage collapse computations using tangent vectors," *IEEE Transactions on Power Systems*, vol. 12, no. 3, pp. 1380-1387, Aug. 1997.

[15] C. A. Canizares, A. C. Z. De Souza, and V. H. Quintana, "Comparison of performance indices for detection of proximity to voltage collapse," *IEEE Transactions on Power Systems*, vol. 11, no. 3, pp. 1441-1450, Aug. 1996.

[16] K. Vu, M. M. Begovic, D. Novosel, and M. M. Saha, "Use of local measurements to estimate voltage-stability margin," *IEEE Transactions on Power Systems*, vol. 14, no. 3, pp. 1029-1035, Aug. 1999.

[17] S. Corsi and G. N. Taranto, "A real-time voltage instability identification algorithm based on local phasor measurements," *IEEE Transactions on Power Systems*, vol. 23, no. 3, pp. 1271-1279, Aug. 2008.

[18] B. Milosevic and M. Begovic, "Voltage-stability protection and control using a wide-area network of phasor measurements," *IEEE Transactions on Power Systems*, vol. 18, no. 1, pp. 121-127, Feb. 2003.

[19] I. Smon, G. Verbic, and F. Gubina, "Local voltage-stability index using tellegen's theorem," *IEEE*

Transactions on Power Systems, vol. 21, no. 3, pp. 1267-1275, Aug. 2006.

[20] F. Hu, K. Sun, A. Del Rosso, E. Farantatos, and N. Bhatt, "Measurement based real-time voltage stability monitoring for load areas," *IEEE Transactions on Power Systems*, vol. 31, no. 4, pp. 2787-2798, Sep. 2016.

[21] H. Yuan, F. Li, H. Cui, X. Lu, D. Shi, and Z. Wang, "A measurement-based VSI for voltage dependent loads using angle difference between tangent lines of load and PV curves," *Electric Power Systems Research*, vol. 160, pp. 13-16, Jul. 2018.

[22] K. P. Guddanti, A. R. R. Matavalam, and Y. Weng, "PMU-based distributed non-iterative algorithm for real-time voltage stability monitoring," *IEEE Transactions on Smart Grid*, vol. 11, no. 6, pp. 5203-5215, Nov. 2020.

[23] A. R. R. Matavalam, S. M. H. Rizvi, A. K. Srivastava, and V. Ajjarapu, "Critical comparative analysis of measurement based centralized online voltage stability indices," *IEEE Transactions on Power Systems*, vol. 37, no. 6, pp. 4618-4629, Nov. 2022.

[24] D. A. Douglass, "Weather-dependent versus static thermal line ratings (power overhead lines)," *IEEE Transactions on Power Delivery*, vol. 3, no. 2, pp. 742-753, Apr. 1988.

[25] IEEE standard for calculating the current-temperature relationship of bare overhead conductors, in: *IEEE Std 738-2012 Revis. IEEE Std 738-2006 - Inc. IEEE Std 738-2012 Cor 1-2013*, 2013, pp. 1-72.

[26] D. A. Douglass, J. Gentle, H.-M. Nguyen, W. Chisholm, C. Xu, T. Goodwin, *et al.*, "A review of dynamic thermal line rating methods with forecasting," *IEEE Transactions on Power Delivery*, vol. 34, no. 6, pp. 2100-2109, Dec. 2019.

[27] R. D. Zimmerman, C. E. Murillo-Sanchez, and R. J. Thomas, "MATPOWER: steady-state operations, planning and analysis tools for power systems research and education," *IEEE Transactions on Power Systems*, vol. 26, no. 1, pp. 12-19, Feb. 2011.

[28] A. Mohamed, G. B. Jasmon, and S. Yusoff, "A static voltage collapse indicator using line stability factors," *Journal of Industrial Technology*, vol. 7, no. 1, pp. 73-85, 1989.

Dumrongsak Wongta received the B.Eng. degree in electrical engineering from Chiangrai College in 2009, and the M.Eng. degree in electrical engineering from University of Phayao in 2017. He is currently a Lecturer at the Department of Electrical Engineering, Faculty of Engineering, Chiangrai College, Thailand. His research interests include applications of artificial intelligence in power system, renewable energy, and state estimation.

Sermsak Uatrongjit received the B.Eng degree in electrical engineering from Chiang Mai University, Thailand, the M.Eng and Ph.D. degrees from the Tokyo Institute of Technology, Japan. He is now an Associate Professor at the Department of Electrical Engineering, Faculty of Engineering, Chiang Mai University. His research interest is in the field of numerical techniques for circuit simulations, optimization, and state estimation.

Chawasak Rakpenthai received the B.Eng., M.Eng. and Ph.D. degrees in electrical engineering from Chiang Mai University in 1999, 2003, and 2007, respectively. He is currently an Associate Professor at the Department of Electrical Engineering, School of Engineering, University of Phayao, Thailand. His research interests include applications of artificial intelligence in power system, power electronics, power system state estimation, and FACTS devices.

Nattapong Pothi received the B.Eng. and M.Eng. degrees in electrical engineering from Chiang Mai university, Chiang Mai, Thailand, in 2003 and 2007, respectively, and the Ph.D. degree in Electronic and Electrical Engineering from University of Sheffield, United Kingdom, in 2016. Since 2007, he has been with the School of Engineering, University of Phayao, Thailand, where he is currently an Assistant Professor in the Department of Electrical Engineering. His research interests include the areas of electric drives, flux-weakening control, energy conversion systems, and power electronic applications.